Int J Thermophys (2010) 31:1904–1918
DOI 10.1007/s10765-008-0544-4

Hot-Ball Method for Measuring Thermal Conductivity

Ľudovít Kubičár · Viliam Vretenár · Vladimír Štofanik · Vlastimil Boháč

Published online: 9 December 2008

Abstract This article deals with the theory and performance of a sensor for measuring thermal conductivity. The sensor, in the form of a small ball, generates heat and simultaneously measures its temperature response. An ideal model of the hollow sphere in an infinite medium furnishes a working equation of the hot-ball method. A constant heat flux through the surface of the ball generates the temperature field. The thermal conductivity of the surrounding medium is to be determined by the stabilized value of the temperature response, i.e., when the steady-state regime is attained. Error components of the sensor are discussed due to analysis of the deviations of the real hot-ball construction from the ideal model. The functionality of a set of hot balls has been tested, and the calibration for a limited range of thermal conductivities was performed. A working range of thermal conductivities of tested materials has been estimated to be from $0.06\,\mathrm{W\cdot m^{-1}\cdot K^{-1}}$ up to $1\,\mathrm{W\cdot m^{-1}\cdot K^{-1}}$.

Keywords Hot-ball method · Sensor · Thermal conductivity · Transient methods

1 Introduction

Over the last 20 years, a new class of transient methods for measuring thermophysical properties has spread in research laboratories as well as in technology. Principal differences between classical and transient methods lie in varieties of specimen size, measuring time, and number of measured parameters. Transient methods need a significantly shorter time for a measurement than classical ones, and moreover, some of them can be used to determine the specific heat, thermal diffusivity, and thermal conductivity within a single measurement [1–3]. Improvements in the methodology

Ľ. Kubičár (✉) · V. Vretenár · V. Štofanik · V. Boháč
Institute of Physics SAV, Dúbravská cesta 9, 845 11 Bratislava, Slovakia
e-mail: kubicar@savba.sk

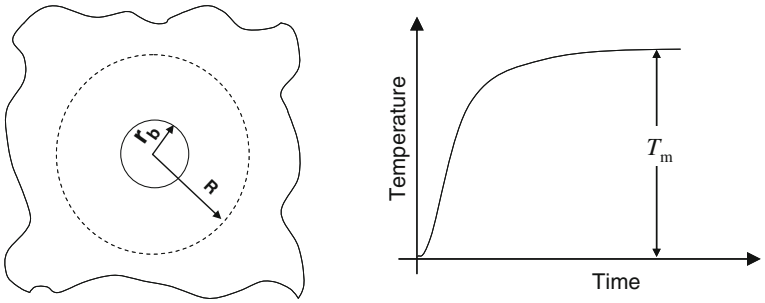

Fig. 1 Sketch of the hot ball (*left*, r_b—radius of the hot-ball sensor, R—heat penetration depth) and temperature response corresponding to its heat output $q = \text{const}$ (*right*)

of transient methods and the use of recent electronic elements allow construction of portable instruments and monitoring systems that significantly simplify operation [4–6]. By now, the needle probe [4] and the hot-bridge [7] sensors have been the most often used in portable instruments. Recently, a description of a hot-ball sensor in a two-function configuration, i.e., as a heat source and thermometer fixed apart from each other, has been published [8].

The present article deals with the hot-ball sensor in a single-function configuration, i.e., a heat source and a thermometer are incorporated in a single unit. The working equation is derived. Disturbing factors like the real properties of the ball and the thermal contact resistance between the ball and the surrounding medium are analyzed. Construction of the hot ball, the peripheral instrumentation, and the measurement methodology are discussed. The calibration based on some reference materials is described. A working range of thermal conductivities of tested materials has been estimated.

2 Principle of the Hot-Ball Sensor

A sketch of an embedded hot-ball sensor is shown in Fig. 1 (left). A heat source in the form of a small ball starts to produce with a constant rate the heat and simultaneously measures the temperature response of the surrounding medium with time (Fig. 1, right). The temperature response stabilizes at a constant value T_m after some time. T_m is used to determine the thermal conductivity of the surrounding medium. Heat penetrates to a sphere of radius R during the temperature stabilization to T_m. Thus, the determined thermal conductivity corresponds to the material within this sphere. Therefore, an average value is to be determined for inhomogenous materials.

3 Working Equation

The working equation of the hot-ball sensor is based on an ideal model. The ideal model assumes a constant heat flux q from the hollow sphere of radius r_b into the infinite medium. Then, the temperature distribution within the medium is characterized by the function [9],

$$T(r,t) = \frac{q}{4\pi r\lambda}\left\{\operatorname{erfc}\left(\frac{r-r_\mathrm{b}}{2\sqrt{at}}\right) - \exp\left(\frac{r-r_\mathrm{b}}{r_\mathrm{b}} + \frac{at}{r_\mathrm{b}^2}\right)\operatorname{erfc}\left(\frac{r-r_\mathrm{b}}{2\sqrt{at}} + \frac{\sqrt{at}}{r_\mathrm{b}}\right)\right\} \tag{1}$$

where $\operatorname{erfc}(x)$ is the complementary error function defined by $\operatorname{erfc}(x) = 1 - \frac{2}{\pi}\int_0^x \exp(-\zeta^2)\mathrm{d}\zeta$, and λ and a are the thermal conductivity and thermal diffusivity of the surrounding medium, respectively. Equation 1 is a solution of the partial differential equation for heat conduction for $r \geq r_\mathrm{b}$ considering the following boundary and initial conditions,

$$\begin{aligned} T(r,t) &= 0, \quad t = 0, \\ \lambda\frac{\partial T(r,t)}{\partial r} &= -\frac{q}{4\pi r_\mathrm{b}^2}, \quad r = r_\mathrm{b}, t > 0. \end{aligned}$$

Assuming that the temperature is measured at the surface of the hollow sphere $r = r_\mathrm{b}$, Eq. 1 is simplified as

$$T(t) = \frac{q}{4\pi r_\mathrm{b}\lambda}\left\{1 - \exp\left(\frac{at}{r_\mathrm{b}^2}\right)\operatorname{erfc}\left(\frac{\sqrt{at}}{r_\mathrm{b}}\right)\right\}. \tag{2}$$

Then for long times ($t \to \infty$), Eq. 2 gives the following working equation of the measuring method:

$$\lambda = \frac{q}{4\pi r_\mathrm{b} T_\mathrm{m}(t \to \infty)} \tag{3}$$

where T_m is the stabilized value of the temperature response. The hollow sphere represents an ideal hot-ball of radius r_b characterized by a vanishing heat capacity. Similar methodology has been applied for deriving the working equation of the hot-wire method [2].

The measuring method based on Eq. 3 belongs, in fact, among the class of transient ones. Nevertheless, heat sources of spherical symmetry possess a special feature, i.e., it yields the steady state at long times, which is utilized to measure the thermal conductivity. To realize an experiment according to the conditions valid for use of Eq. 3, one needs

- to construct a hot-ball sensor composed of real materials,
- to find the time period when the steady-state regime is attained,
- to analyze the real properties of the hot ball.

4 Hot-Ball Real Properties

A hot ball must be constructed of parts generating a constant rate of heat on the one hand and measuring the temperature response on the other hand. Theoretical analysis of such a hot-ball structure requires a sophisticated mathematical approach that might

not always provide the expected information. Due to close limits in theory, we accept simplified models of the hot ball represented by a homogenous material ascribed to the heater as well as to the thermometer. Models will be analyzed that characterize transient and steady-state regimes.

4.1 Transient Regime of the Real Hot Ball

Assuming that the hot ball is a perfect thermal conductor, the measured temperature can be ascribed to its surface temperature. Such a device has its own non-vanishing heat capacity causing a deviation from the ideal model, Eq. 1. A model including the heat capacity of the ball Mc^* and the thermal contact resistance $1/H$ between the hot ball and the surrounding medium is characterized by the function [10],

$$T_\mathrm{b}(t) = \frac{q}{4\pi\lambda r_\mathrm{b}}\left[\frac{1+r_\mathrm{b}h}{r_\mathrm{b}h} - \frac{2r_\mathrm{b}^2 f^2 h^2}{\pi}\int_0^\infty \frac{\exp\left(-au^2 t/r_\mathrm{b}^2\right)}{\left[u^2\left(1+r_\mathrm{b}h\right) - fr_\mathrm{b}h\right]^2 + \left(u^3 - fr_\mathrm{b}hu\right)^2}\mathrm{d}u\right] \tag{4}$$

where $f = 4\pi r_\mathrm{b}^3 \rho \frac{c}{Mc^*}$, q is the heat supplied over the surface at $r = r_\mathrm{b}$, M is the mass and c^* is the specific heat of the hot ball, c, ρ are the specific heat and density of the medium, respectively, and $h = H/\lambda$. H is the thermal contact conductance. Equation 4 is a solution of the partial differential equation for heat conduction considering the boundary and initial conditions,

$$\begin{aligned}
&T_\mathrm{b}(t) = T_\mathrm{med}(r,t) = 0, \quad t = 0,\\
&\lambda\frac{\partial T_\mathrm{med}(r,t)}{\partial t} + H\left(T_\mathrm{b}(t) - T_\mathrm{med}(r,t)\right) = 0, \quad r = r_\mathrm{b}, t > 0,\\
&H\left(T_\mathrm{b}(t) - T_\mathrm{med}(r,t)\right)4\pi r_\mathrm{b}^2 + Mc^*\frac{\partial T_\mathrm{b}(t)}{\partial t} = q, \quad r = r_\mathrm{b}, t > 0.
\end{aligned}$$

where T_med is the surface temperature of the surrounding medium. The heat capacity of the hot ball Mc^* and the thermal contact resistance $1/H$ affects the transient response and thus, it influences the measuring process.

4.2 Hot-Ball Heat Capacity

For good thermal contact ($H \to \infty$), Eq. 4 can be rewritten in a form,

$$T_\mathrm{cap}(t) = \frac{q}{4\pi\lambda r_\mathrm{b}}\left[1 - \frac{2r_\mathrm{b}^2 f^2}{\pi}\int_0^\infty \frac{\exp\left(-au^2 t/r_\mathrm{b}^2\right)}{\left(u^2 r_\mathrm{b} - fr_\mathrm{b}\right)^2 + \left(fr_\mathrm{b}u\right)^2}\mathrm{d}u\right] \tag{5}$$

that is used for analysis of the influence of the hot-ball heat capacity on the measuring process for a range of hot-ball heat capacities Mc^*. The analysis gives the

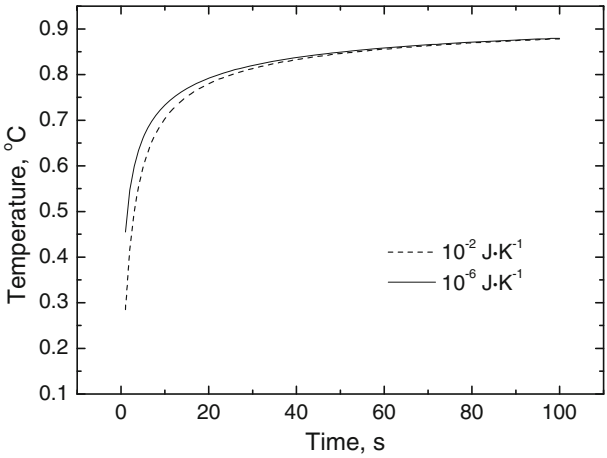

Fig. 2 Transients calculated using Eq. 5. Parameter: heat capacity of the hot ball, Mc^*

results shown in Fig. 2 for parameters of the hot ball: heat output $q = 6\,\mathrm{mW}$, radius $r_\mathrm{b} = 1\,\mathrm{mm}$, and of the tested polymeric material: density $\rho = 1,000\,\mathrm{kg \cdot m^{-3}}$, thermal conductivity $\lambda = 0.5\,\mathrm{W \cdot m^{-1} \cdot K^{-1}}$, and thermal diffusivity $a = 0.5\,\mathrm{mm^2 \cdot s^{-1}}$. A negligible influence of the heat capacity of the hot ball has been found in a broad range from $10^{-6}\,\mathrm{J \cdot K^{-1}}$ to $10^{-2}\,\mathrm{J \cdot K^{-1}}$. A criterion of the steady state has been searched due to calculation of a transient, Eq. 5, considering the hot-ball heat capacity $Mc^* = 4 \times 10^{-5}\,\mathrm{J \cdot K^{-1}}$ and the above given parameters. The working equation, Eq. 3, has been used for thermal conductivity evaluation point-by-point using the calculated transient as input data. A 5 % deviation $(0.5 - \lambda_\mathrm{calc})100/0.5$ from the thermal-conductivity input $\lambda = 0.5\,\mathrm{W \cdot m^{-1} \cdot K^{-1}}$ has been found after 65 s. Deviations can be reduced using a longer measuring time. This test shows the steady-state regime can be attained after 65 s for materials of thermal diffusivity $a = 0.5\,\mathrm{mm^2 \cdot s^{-1}}$.

4.3 Thermal Contact

We look at the effect of the thermal contact of the hot ball with the surrounding medium. For a negligible hot-ball heat capacity ($Mc^* \to 0$), Eq. 4 can be rewritten in a form,

$$T_\mathrm{H}(t) = \frac{q}{4\pi\lambda r_\mathrm{b}} \left[\frac{1 + r_\mathrm{b}h}{r_\mathrm{b}h} - \frac{2r_\mathrm{b}^2h^2}{\pi} \int_0^\infty \frac{\exp\left(-au^2t/r_\mathrm{b}^2\right)}{r_\mathrm{b}^2h^2\left(1+u^2\right)} \mathrm{d}u \right] \tag{6}$$

An analysis of the effect of the thermal contact has been performed using the hot-ball radius $r_\mathrm{b} = 1\,\mathrm{mm}$, heat output $q = 6\,\mathrm{mW}$, and thermophysical parameters of the medium density, $\rho = 1,000\,\mathrm{kg \cdot m^{-3}}$, thermal conductivity $\lambda = 0.5\,\mathrm{W \cdot m^{-1} \cdot K^{-1}}$, and thermal diffusivity $a = 0.5\,\mathrm{mm^2 \cdot s^{-1}}$ for different thermal contact conductances H. A rather strong influence of the thermal contact conductance on the transient has been

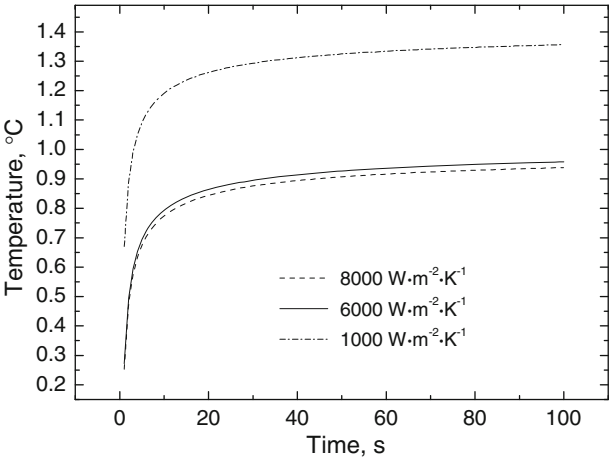

Fig. 3 Transients calculated using Eq. 6. Parameter: thermal contact conductance, H

found (see Fig. 3) for $H < 6{,}000\,\mathrm{W \cdot m^{-2} \cdot K^{-1}}$. The transients influenced by the thermal contact are shifted to higher values, even if its shape has not changed. A test of the steady-state regime has, again, shown that the time period to obtain stable data for the thermal conductivity within 5 % takes 65 s for polymers having a thermal diffusivity $a = 0.5\,\mathrm{mm^2 \cdot s^{-1}}$. However, data for the thermal conductivity are shifted to lower values.

4.4 Steady-State Regime

The previous analysis is based on the assumption that the hot ball is a perfect heat conductor. This corresponds to an experimental setup, where the difference in thermal conductivity of the hot ball and of the surrounding medium is large. However, a variation of the hot-ball properties is limited due to the properties of its components. Therefore, we look for a thermal conductivity range of the tested materials considering the real properties of the hot ball. As the transient properties are discussed in the previous paragraphs, the steady-state regime is now to be analyzed. We look for the temperature distribution within the ball, across the contact as well as within the surrounding medium. In general, the hot ball and surrounding medium represent different materials. A solution of the partial differential equation that includes constant heat production has the form [11],

$$T_\mathrm{b}(r) = q\,\frac{\left[r_\mathrm{b}^2 - r^2 + \frac{2}{H} r_\mathrm{b}\lambda_\mathrm{b} + 2r_\mathrm{b}^2\left(\frac{\lambda_\mathrm{b}}{\lambda}\right)\right]}{8\pi\lambda_\mathrm{b} r_\mathrm{b}^3} \quad \text{for } r \le r_\mathrm{b} \tag{7}$$

and

$$T(r) = \frac{q}{4\pi r\lambda} \quad \text{for } r \ge r_\mathrm{b}, \tag{8}$$

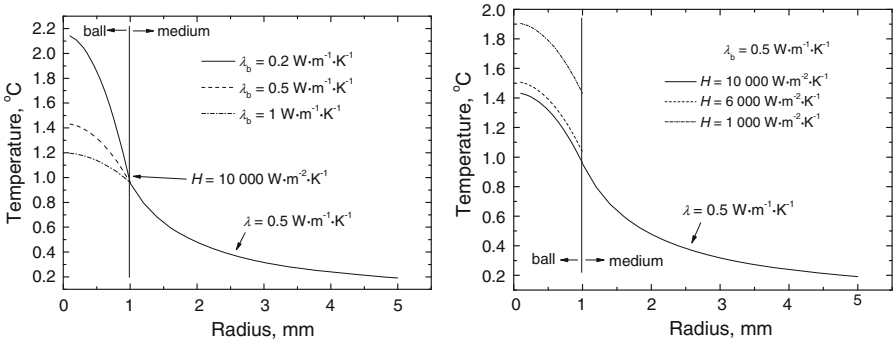

Fig. 4 Temperature distributions within the hot ball and inside the surrounding medium. Parameters: thermal conductivity of the hot ball, λ_b, and surrounding medium, λ, and the thermal contact conductance between the hot ball and the medium, H

where $T_b(r)$ and $T(r)$ characterize temperature distributions within the hot ball and the medium, respectively, H is the thermal contact conductance, and r_b and λ_b are the radius and thermal conductivity of the hot ball, respectively.

The functions, Eqs. 7 and 8, have been found by a solution of the partial differential equation for heat conduction considering the following boundary conditions:

$$\lambda_b \frac{\partial T_b(r)}{\partial r} = \lambda \frac{\partial T_{med}(r)}{\partial r}, \quad r = r_b,$$
$$\lambda \frac{\partial T_{med}(r)}{\partial r} + H(T_b(r) - T_{med}(r)) = 0, \quad r = r_b,$$
$$\lambda_b \frac{\partial T_b(r)}{\partial r} = \frac{-qr}{4\pi r_b^3}, \quad r \le r_b.$$

Influence of the hot-ball properties on the temperature distribution within the hot ball, across the contact, and within the surrounding medium has been analyzed using Eqs. 7 and 8 for different materials of the hot ball (thermal conductivity range λ_b from $0.2\,\mathrm{W\cdot m^{-1}\cdot K^{-1}}$ up to $1\,\mathrm{W\cdot m^{-1}\cdot K^{-1}}$) and enough high thermal contact conductance $H = 10{,}000\,\mathrm{W\cdot m^{-2}\cdot K^{-1}}$ to suppress its influence on the measuring process (Fig. 4, left). The surrounding medium has a thermal conductivity $\lambda = 0.5\,\mathrm{W\cdot m^{-1}\cdot K^{-1}}$. The hot-ball radius is 1 mm, and the heat output $q = 6$ mW. The shape of the profile inside the hot ball depends on its thermal conductivity. The temperature distribution in the medium is not influenced by variations of the thermal properties of the hot ball. This follows from Eq. 8. For data evaluation one needs a surface temperature of the medium (see Eq. 3), while the real hot ball gives the volume ball temperature considering its construction. There is a difference between the medium surface temperature and the volume hot-ball temperature that causes a data shift. This can be recognized as a systematic measurement error. The smallest difference between the medium surface temperature and the volume hot-ball temperature is observed for a material having a thermal conductivity $\lambda_b \ge 1\,\mathrm{W\cdot m^{-1}\cdot K^{-1}}$.

The effect of the non-ideal contact has been analyzed using Eqs. 7 and 8 for the hot ball and the surrounding medium that are characterized by thermal conductivities

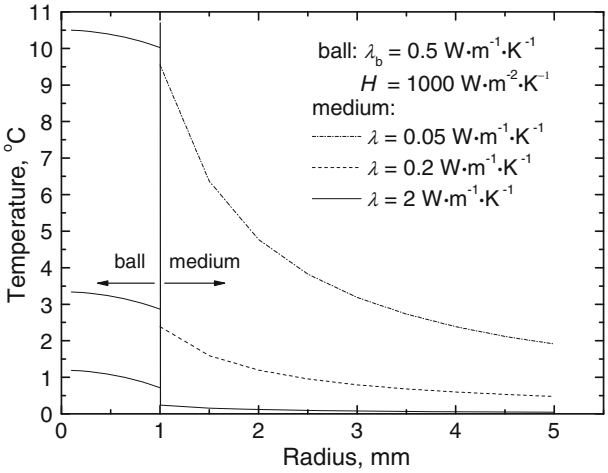

Fig. 5 Temperature distributions within the hot ball and inside the surrounding medium for different thermal conductivities of the surrounding materials. Parameters: thermal conductivity of the hot ball, λ_b, and surrounding medium λ, and the thermal contact conductance between the hot ball and the medium, H

$\lambda_b = 0.5\,\mathrm{W \cdot m^{-1} \cdot K^{-1}}$ and $\lambda = 0.5\,\mathrm{W \cdot m^{-1} \cdot K^{-1}}$ assuming a hot-ball radius $r_b = 1$ mm and heat output $q = 6$ mW. The non-ideal thermal contact was characterized by a set of thermal contact conductances, namely, $H = 1{,}000\,\mathrm{W \cdot m^{-2} \cdot K^{-1}}$, $6{,}000\,\mathrm{W \cdot m^{-2} \cdot K^{-1}}$, and $10{,}000\,\mathrm{W \cdot m^{-2} \cdot K^{-1}}$. Results are shown in Fig. 4 (right). Variations in the quality of the thermal contact have no influence on the temperature profiles within the hot ball and the surrounding medium; however, the temperature profiles within the hot ball are shifted to higher values depending on the thermal contact conductance. Using Eq. 3 for data evaluation, one finds an additional data shift due to differences between the volume ball temperature and the medium surface temperature. Again, this can be recognized as a systematic measurement error.

Two disturbing effects have been discussed, namely, the effect of the real hot-ball properties and the effect of the thermal contact resistance. Both effects cause a temperature difference between the volume hot-ball temperature and the medium surface temperature that leads to systematic measurement error when using Eq. 3 for data evaluation. We look for the impact of both effects upon data when materials are tested over a broad range of thermal conductivity. Results of the analysis are shown in Fig. 5. Data are calculated using Eqs. 7 and 8 for the hot-ball thermal conductivity $\lambda_b = 0.5\,\mathrm{W \cdot m^{-1} \cdot K^{-1}}$, thermal contact conductance $H = 1{,}000\,\mathrm{W \cdot m^{-2} \cdot K^{-1}}$, and a surrounding medium of a set of thermal conductivities $\lambda = 0.05\,\mathrm{W \cdot m^{-1} \cdot K^{-1}}$, $0.2\,\mathrm{W \cdot m^{-1} \cdot K^{-1}}$, and $2\,\mathrm{W \cdot m^{-1} \cdot K^{-1}}$. A hot-ball radius $r_b = 1$ mm and a heat output $q = 6$ mW were used in the calculations. The temperature profile within the ball and the temperature drop at the contact is the same, i.e., the temperature shift is the same for all thermal conductivities of the surrounding medium. Thus, a correction based on calibration of the sensor using standard materials can be introduced. The temperature profile within the medium is strongly influenced by its thermal conductivity. Due to the high temperature increase at the medium surface, the role of this temperature

shift is suppressed for low thermal-conductivity materials. In addition, the temperature distribution within the ball is negligible when low thermal-conductivity materials are tested. Thus, measurements of the low thermal-conductivity materials can be provided with higher precision.

5 Experiments

A hot-ball sensor has been constructed consisting of two elements, a heater and a thermometer (patent pending). Both elements are fixed in the ball using epoxy resin. The diameter of the hot ball ranges from 2 mm to 2.3 mm. A simple instrument was constructed that consists of a data logger, a microcontroller connected with an A/D converter for temperature measurements, and a D/A converter associated with the current source for heat generation. The instrument can be pre-programmed through a USB channel by a PC.

The strategy of the experimental validation of the theory is based on the calibration of hot-ball sensors. Equation 3 is rewritten in a form,

$$q/T_{\mathrm{m}} = 4\pi r_{\mathrm{b}}\lambda = A\lambda \tag{9}$$

where A is a constant defined as $A = 4\pi r_{\mathrm{b}}$. The ratio q/T_{m} is a linear function of thermal conductivity that will be tested using certified reference materials. Here, these materials include the ones tested within an intercomparison of different labs and various methods. In principle, the hot-ball sensor might be an absolute method for measuring the thermal conductivity providing that the assumptions given by the theory are satisfied. In addition, Eq. 9 will be plotted using the ball radius $r_{\mathrm{b}} = 1.05$ mm. The sensor is made of real materials and the thermal contact between the sensor and the surrounding medium causes a data shift; thus, a calibration of every sensor is required. A difference between the experimental data and the theoretical function (Eq. 9) should indicate the significance of the thermal contact resistance and the temperature gradient within the ball.

A phenolic foam, aerated concrete, calcium silicate, PMMA, and Sander sandstone were used for calibration experiments. Table 1 gives the basic characteristics of the tested materials along with the experimental parameters used. Each tested specimen consists of two blocks, and the sensor is placed in contact between two specimen surfaces. To improve the thermal contact, a groove was machined into one specimen block into which the hot ball was placed. In addition, contact paste (Middland Silicones Ltd) was used. While testing a porous structure, the contact surfaces were covered by epoxy varnish to prevent the paste from diffusing into the material.

A typical measurement signal is shown in Fig. 6 along with the characteristic points used for the calculation of the thermal conductivity. The measuring procedure consists of the specimen temperature measurement representing the baseline, switching-on the heating, and simultaneously scanning the hot-ball temperature. When the hot-ball temperature has stabilized, the heating is interrupted, and a period of temperature equilibration follows. After equilibration, the next run may be performed. The

Table 1 Materials and experimental parameters for calibration of a hot-ball sensor

Material	Thermal conductivity ($W \cdot m^{-1} \cdot K^{-1}$)	Structure	q (mW)	Measuring period (s)	Block size (mm^3)
Sandstone [12]	1.9	Porous	6.5	19	$50 \times 50 \times 20$
PMMA [13,14]	0.19	Compact	2.5	380	$\phi 50$, Length 25
Aerated concrete [15,16]	0.155	Porous, anisotropic	2.5	240	$150 \times 150 \times 50$
Calcium silicate [17]	0.097	Porous	1.5	240	$150 \times 150 \times 50$
Phenolic foam [18]	0.06	Porous	1.5	336	$150 \times 150 \times 50$

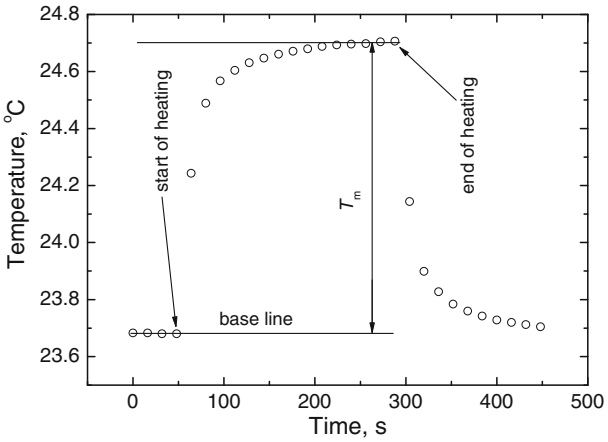

Fig. 6 Measuring cycle. Material: aerated concrete, hot-ball output $q = 3.5\,\text{mW}$

repetition rate of the measurements depends on the thermal diffusivity, and it varies from 10 min to 60 min.

5.1 Results

Tests of the measurement reliability using aerated concrete have been performed varying the hot-ball heat output over a broad range. The ball radius $r_b = 1.05\,\text{mm}$ has been used. The results are shown in Fig. 7 (left). Data for the thermal conductivity remain steady in the range from 2.5 mW to 30 mW within $\Delta\lambda = \pm 0.0007\,\text{W} \cdot \text{m}^{-1} \cdot \text{K}^{-1}$. The measured data are shifted to higher values (compare Fig. 7 with Table 1). The shift is constant within a broad range of the hot-ball heat output. The data shift reached $\Delta\lambda = 0.179\,\text{W} \cdot \text{m}^{-1} \cdot \text{K}^{-1}$. The test has shown that the measured data are not influenced by the hot-ball heat output as long as $q \geq 2.5\,\text{mW}$.

A test of the steady-state regime has been made using PMMA and measuring parameters $q = 2.5\,\text{mW}$, ball radius $r_b = 1.05\,\text{mm}$, and a measuring period (heating time) of 3,000 s. The scanned temperature along with the calculated thermal conductivity is

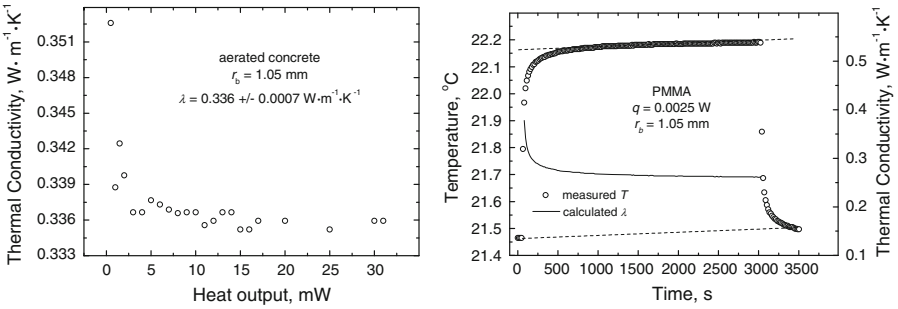

Fig. 7 Thermal conductivity of aerated concrete as a function of the hot-ball heat output (*left*). Temperature response and thermal conductivity of the PMMA as a function of time (*right*)

shown in Fig. 7 (right). Equation 3 was used for data evaluation, point-by-point, of the scanned temperature response (300 points). A small temperature increase was found after the heating was switched off. Therefore, the baseline was approximated by a line that connects the 3rd and 210th points. Then, the temperature T_{m}, included in the calculation, is established as a difference between this baseline and the corresponding point of the temperature response after the start of heating. Data on the thermal conductivity started to be stable after 500 s and, again, shifted to higher values. The data shift reached $\Delta\lambda = 0.17\,\mathrm{W}\cdot\mathrm{m}^{-1}\cdot\mathrm{K}^{-1}$ and this shift is nearly the same as for aerated concrete.

Sensors are not of a regular ball shape; therefore, one may assume that data may be scattered comparing individual sensors. In addition, the groove made in the used materials is also not of a regular shape. Therefore, in order to obtain an overview on data statistics, the following strategy of the experiment has been chosen. Eight different sensors were tested. At least five runs at a fixed setup and two re-assemblings have been realized for every sensor/material configuration. A re-assembling consists of cleaning the groove, deposition of the contact paste at the groove point where the ball is fixed, fixing the ball into the groove, and assembling both parts of the tested materials together into one unit. Data obtained on a set of materials specified in Table 1 are shown in Fig. 8.

Analysis of data statistics has shown that the measurement reproducibility of the assembled specimen setup is high. Data scatter is well below 1 %. Reassembling introduces data scatter within (3 to 5) %. The largest contribution to data scatter has been obtained with a combination of re-assembling and use of different sensors. The corresponding error bars are shown in Fig. 8. Two types of sensors marked as HB3xx (see Fig. 9 left—upper photo) and HB4xx (see Fig. 9 left—lower photo) have been included in the calibration. The dashed line represents a calibration function. The thermal conductivity of the tested material can be determined by measuring the stabilized temperature response T_{m} due to the hot-ball heat output q and using the calibration function (dashed line).

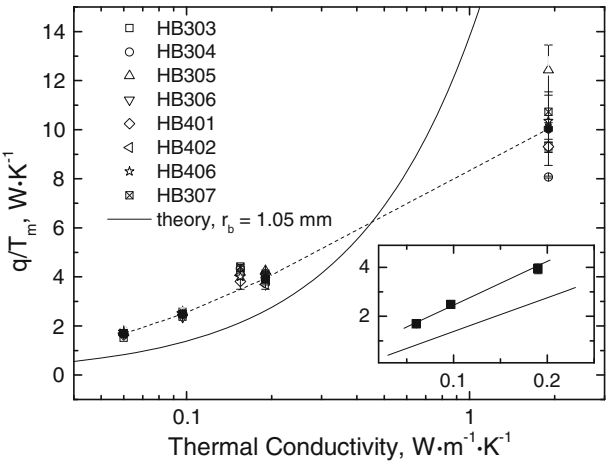

Fig. 8 Calibration function of hot-ball sensors. The solid line follows the ideal model (Eq. 9) using ball radius $r_b = 1.05$ mm. The inset shows the thermal conductivity range where q/T_m is a linear function of the thermal conductivity, $q/T_m = 0.6728 + 17.842\lambda$

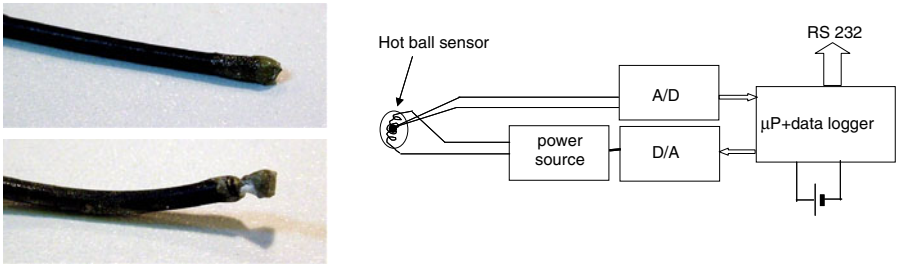

Fig. 9 Photos of two hot-ball sensors prepared in different designs (*left*). Schematic of instrumentation for measuring thermal conductivity by the hot-ball method (*right*)

6 Discussion

A theoretical curve (solid line) is plotted in Fig. 8 using Eq. 9, where the ball radius is assumed to be $r_b = 1.05$ mm. A data shift to higher values (a difference between the experimental and theoretical values) can be found for the low thermal-conductivity range and to lower ones for the high thermal-conductivity range. The inset in Fig. 8 shows the range of the thermal conductivity where the sensor follows the ideal model; however, data are systematically shifted to higher values. To analyze the possible sources of the data shift, Eq. 3 is rewritten in a form,

$$\lambda_{app} = \frac{q_o + q_w}{4\pi r_b (T_m + \delta T_b + \delta T_c)} = \lambda \frac{\left(1 + \frac{q_w}{q_o}\right)}{\left(1 + \frac{\delta T_b}{T_m} + \frac{\delta T_c}{T_m}\right)}, \tag{10}$$

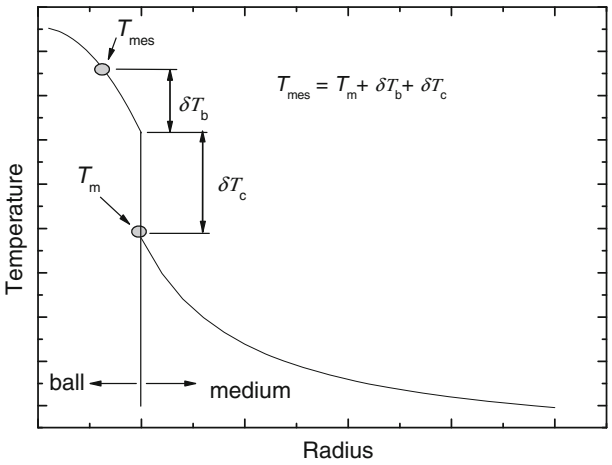

Fig. 10 Temperature distribution within the hot ball, thermal contact, and the medium during the experiment

where λ follows the ideal model (Eq. 3) considering the hot-ball heat output q_o, $q = q_w + q_o$ is the overall hot-ball heat output, δT_b is the temperature drop across the radius of the hot ball, δT_c is the temperature drop at the thermal contact, and q_w is the heat loss through the connecting wires. A temperature T_m and a hot-ball heat output q_o have to be used in Eq. 3 to obtain the correct data (see Fig. 10).

Two limiting cases can be found considering Eq. 10. When high thermal-conductivity materials are measured, the apparent thermal conductivity, the lower value λ_{app} in comparison to the real one λ, is calculated due to the significant contribution of both temperature drops, a drop within the hot ball and a drop at the contact (see Fig. 10). The heat loss q_w is negligible as heat transport from the hot-ball to the surrounding medium is highly effective. In addition, a variable thermal contact is achieved due to reassembling. This is a case of sandstone where data on thermal conductivity are shifted down (see Fig. 8) and, in addition, high data scatter is found. Generally, the higher is the thermal conductivity of the medium, the stronger is the influence of the thermal contact on the measuring process. This is shown in Fig. 8 for sandstone data where the error bar increases when a higher thermal-conductivity material is tested.

An opposite situation can be found when low thermal-conductivity materials are measured. Then both temperature drops, a drop within the hot ball and a drop at the contact are negligible, but the heat loss through the wires q_w starts to play a role in the measuring process. This effect shifts the calculated thermal conductivity to higher values.

The hot ball and thermal contact properties as well as heat loss through the connecting wires have been estimated using Eqs. 3, 7, 8, and 10 and scans of the temperature response from experiments on sandstone and PMMA. While the measuring process in the case of sandstone is influenced by the hot ball and contact properties, the heat loss through the contact wires affects the experiment in the case of PMMA.

Considering data obtained by hot-ball sensor HB402 (radius $r_b = 1.1$ mm) on sandstone and using a heat output $q = 6$ mW and a measuring time 11 s, one obtains the

temperature response $T_m = 0.676\,°C$. Using Eq. 3 and $q/T_{meas} = 8.875\,mW \cdot K^{-1}$ one obtains an apparent thermal conductivity $\lambda_{app} = 0.6424\,W \cdot m^{-1} \cdot K^{-1}$. Using the real thermal conductivity of sandstone $\lambda = 1.9\,W \cdot m^{-1} \cdot K^{-1}$ (Table 1), one obtains the theoretical value $q_o/T_m = 26.26\,mW \cdot K^{-1}$ (see Fig. 8). We assume that the heat loss through the connecting wires is negligible $q_w \to 0$ due to the high thermal conductivity of sandstone. Using Eq. 10, one obtains $\delta T_b + \delta T_c = 1.96 T_m$ that yields $\delta T_b + \delta T_c = 0.449\,°C$ while the theoretical temperature response corresponding to point T_m shown in Fig. 10 has a value $T_m = 0.229\,°C$. Thus, the hot ball and thermal contact properties strongly influence the resulting value of the thermal conductivity. Using Eqs. 7 and 8, one can estimate the thermal contact conductance H. Assuming that the hot ball operates in a regime of a nearly perfect conductor, the thermal contact conductance is approximately $H = 160\,W \cdot m^{-2} \cdot K^{-1}$. The estimated value is too low. However, data scatter of the thermal conductivity indicates that the thermal contact plays a prominent role. In addition, the thermal conductivity of the hot ball is about $\lambda_b \sim 1\,W \cdot m^{-1} \cdot K^{-1}$, which is comparable to sandstone. Thus, one needs to also include the thermal properties of the hot ball in the analysis. Then the resultant thermal contact conductance would be higher.

It has been assumed that for the PMMA experiment the hot-ball and thermal contact properties do not influence the measuring process, i.e., $\delta T_b/T_m + \delta T_c/T_m \to 0$ and the heat loss through the connecting wires affects the measuring process. Using the hot-ball heat output $q = 2.5\,mW$ and a measuring time of 320 s, one obtains for the temperature response $T_m = 0.731\,°C$. Using Eq. 3 and $q/T_{meas} = 3.42\,mW \cdot K^{-1}$ one obtains the apparent thermal conductivity $\lambda_{app} = 0.248\,W \cdot m^{-1} \cdot K^{-1}$. Using the real thermal conductivity of PMMA $\lambda = 0.19\,W \cdot m^{-1} \cdot K^{-1}$ (Table 1), one obtains the theoretical value $q_o/T_m = 2.622\,mW \cdot K^{-1}$ (see Fig. 8). Using Eq. 10, one obtains $q_w = 0.576\,mW$ and the theoretical hot-ball heat output corresponding to point T_m shown in Fig. 10 has a value $q_o = 1.9\,mW$. Thus, the connecting wires to the hot ball represent a significant factor shifting the data for thermal conductivity to higher values.

Measurement accuracy by a hot-ball method requires a more detailed experimental as well as a theoretical analysis. While experimentation with different diameters of the connecting wires may help to optimize the hot-ball method for testing low thermal-conductivity materials, a new approach has to be worked out for measurement of high thermal-conductivity materials where the thermal contact resistance plays a predominant role.

7 Conclusions

A new hot-ball sensor for measuring thermal conductivity has been presented. The underlying theory is based on delivering a constant rate of heat flow by a heat source in the form of a ball into an unbounded surrounding medium. The thermal conductivity of the surrounding medium is to be determined by stabilized value of the temperature response, i.e., when the steady-state regime is attained. A working equation of the hot ball based on a model of the hollow sphere in an infinite medium has been found. Theoretical analysis of the disturbing effects on the measuring process, i.e., the real

properties of the hot ball and the thermal contact between the ball and the surrounding medium has been performed. Error components of a measurement are discussed that include disturbing effects and the heat loss through connecting wires.

A hot-ball sensor has been constructed consisting of two elements, a heater and a thermometer. Both elements are fixed in the ball using epoxy resin. The diameter of the hot ball ranges from 2 mm to 2.3 mm. A verification of the theory has been performed using a set of sensors placed in a range of materials having thermal conductivities from $0.06\,\mathrm{W}\cdot\mathrm{m}^{-1}\cdot\mathrm{K}^{-1}$ to $1.9\,\mathrm{W}\cdot\mathrm{m}^{-1}\cdot\mathrm{K}^{-1}$. Analysis of data statistics has shown that the measurement reproducibility of the assembled specimen setup is high. Data scatter is well below 1 %. Reassembling introduces data scatter within 3–5 %. The largest contribution to data scatter ($<\pm 7\,\%$) has been obtained with a combination of re-assembling and use of different sensors.

Experiments have shown that the steady-state regime depending on thermal diffusivity can be reached within 60 s for sandstone ($a = 1.03\,\mathrm{mm}^2\cdot\mathrm{s}^{-1}$) and 500 s for PMMA ($a = 0.12\,\mathrm{mm}^2\cdot\mathrm{s}^{-1}$) considering an acceptable data scatter within 5 %. A calibration can be performed for every specific hot-ball sensor to obtain acceptable precision within 5 %. Additional study needs to be performed to evaluate the measurement uncertainty in detail.

Acknowledgments This work has been supported by the EU project G6RD-CT2000-00266 and by VEGA project 2/5100/25.

References

1. J. Krempaský, Meranie termofyzikálnych veličín (Vyd. SAV, Bratislava, 1969), pp. 1–288 [in Slovak]
2. Ľ. Kubičár, V. Boháč, Review of several dynamic methods of measuring thermophysical parameters, in *Proceedings of 24th International Conference on Thermal Conductivity/12th International Thermal Expansion Symposium*, ed. by P.S. Gaal, D.E. Apostolescu (Technomic Pub. Co., Lancaster, PA, 1999), pp. 135–149
3. Ľ. Kubičár, Pulse method of measuring basic thermophysical parameters, in *Comprehensive Analytical Chemistry, vol. XII, Thermal Analysis, Part E*, ed. by G. Svehla (Elsevier, Amsterdam, Oxford, New York, Tokyo, 1990), pp. 1–350
4. N. Lockmuller, J. Redgrove, Ľ. Kubičár, High Temp. High Press. **35–36**, 127 (2003/2004)
5. http://www.transientms.com
6. R. Model, R. Stosch, U. Hammerschmidt, Int. J. Thermophys. **28**, 1447 (2007)
7. U. Hammerschmidt, W. Sabuga, Int. J. Thermophys. **21**, 1255 (2000)
8. H. Zhang, L. He, S. Cheng, Z. Zhai, D. Gao, Meas. Sci. Technol. **14**, 1396 (2003)
9. H.S. Carslaw, J.C. Jaeger, *Conduction of Heat in Solids* (Clarendon Press, Oxford, 1956), p. 248
10. H.S. Carslaw, J.C. Jaeger, *Conduction of Heat in Solids* (Clarendon Press, Oxford, 1956), p. 349
11. H.S. Carslaw, J.C. Jaeger, *Conduction of Heat in Solids* (Clarendon Press, Oxford, 1956), p. 232
12. L. Kubičár, V. Vretenár, V. Boháč, P. Tiano, Int. J. Thermophys. **27**, 220 (2006)
13. M. J. Assael, K. D. Antoniadis, J. Wu, Int. J. Thermophys. **29**, 1257 (2006)
14. V. Boháč, Ľ. Kubičár, V. Vretenár, in *Proceedings of TEMPMEKO 2004, 9th International Symposium on Temperature and Thermal Measurements in Industry and Science*, ed. by D. Zvizdić, L.G. Bermanec, T. Veliki, T. Stašič (FSB/LPM, Zagreb, Croatia, 2004), pp. 1299–1306
15. P. Matiašovský, O. Koronthályová, Build. Res. J. **42**, 265 (1994)
16. S. Goual, A. Bali, M. Qu/eneudec, J. Phys. D. Appl. Phys. **32**, 3041 (1999)
17. O. Koronthályová, P. Matiašovský, Build. Res. J. **50**, 289 (2002)
18. Ľ. Kubičár, V. Boháč, V. Vretenár, Thermophysical parameters of phenolic foam measured by the pulse transient method: methodology for low thermal conductivity materials, in *Proceedings of 27th International Conference on Thermal Conductivity/15th International Thermal Expansion Symposium*, ed. by H. Wang, W. Porter (DEStech Publications, Inc., Lancaster, PA, 2005), p. 328